

## Supplementary materials

### In-situ Space-Confining Growth of $\text{Co}_3\text{O}_4$ Nanoparticles Inside N-Doped Hollow Porous Carbon Nanospheres as Bifunctional Oxygen Electrocatalysts for High-performance Rechargeable Zinc-Air Batteries

Jingbiao Kuang<sup>a</sup>, Nengfei Yu<sup>a,\*</sup>, Zhongtang Yang<sup>a</sup>, Yi Zhang<sup>a</sup>, Lifei Ji<sup>b</sup>, Jilei Ye<sup>a,\*</sup>, Wen Huang<sup>b</sup>, Qinghong Huang<sup>a</sup>, Na Tian<sup>b</sup>, Yuping Wu<sup>a</sup> and Shigang Sun<sup>b</sup>

<sup>a</sup> School of Energy Science and Engineering, Nanjing Tech University, Nanjing, 211816, China

<sup>b</sup> State Key Laboratory of Physical Chemistry of Solid Surfaces, College of Chemistry and Chemical Engineering, Xiamen University, Xiamen 361005, China

E-mail: yunf@njtech.edu.cn; yejilei@njtech.edu.cn

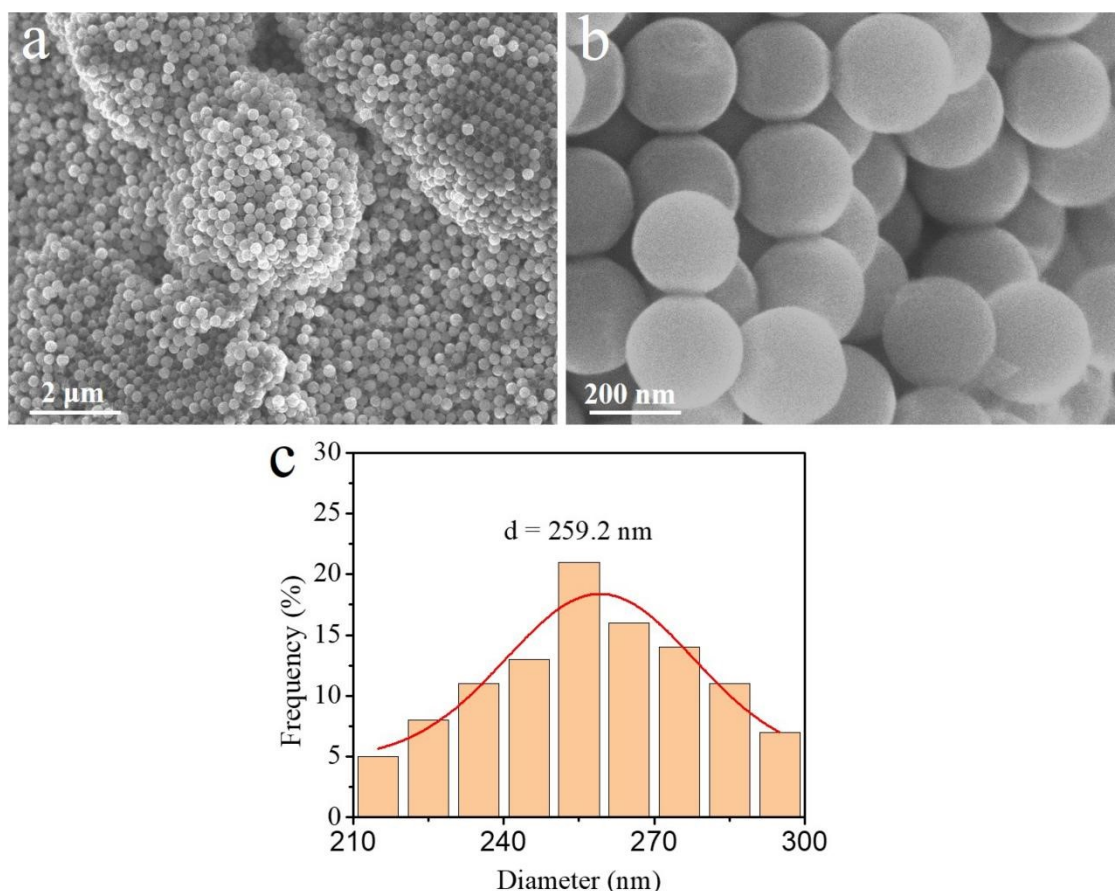


**Figure S1.** a) FESEM and b) enlarged FESEM images of  $\text{SiO}_2$  nanospheres. c) size distribution of  $\text{SiO}_2$  nanospheres

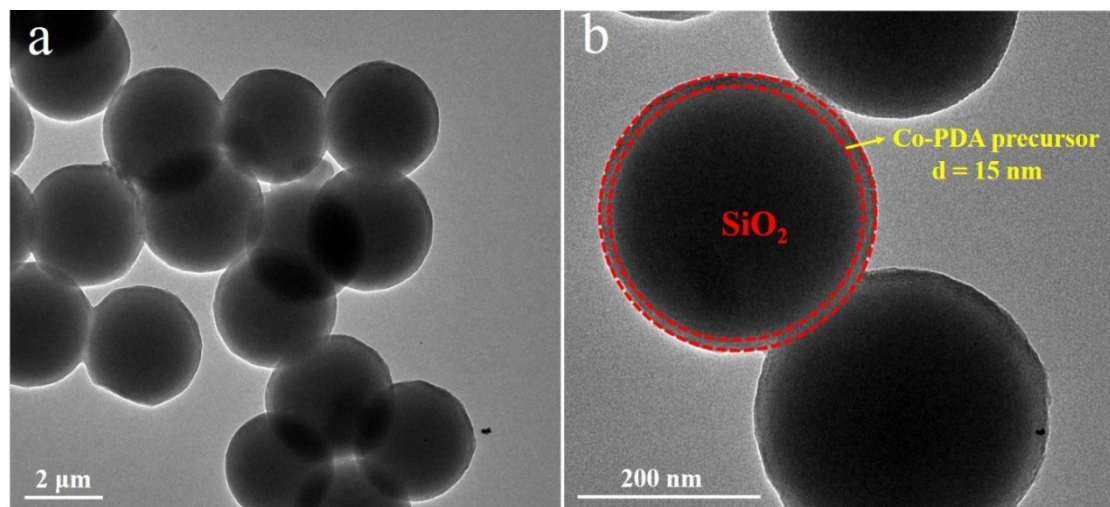


**Figure S2.** TEM images of SiO<sub>2</sub>@Co-PDA nanospheres.

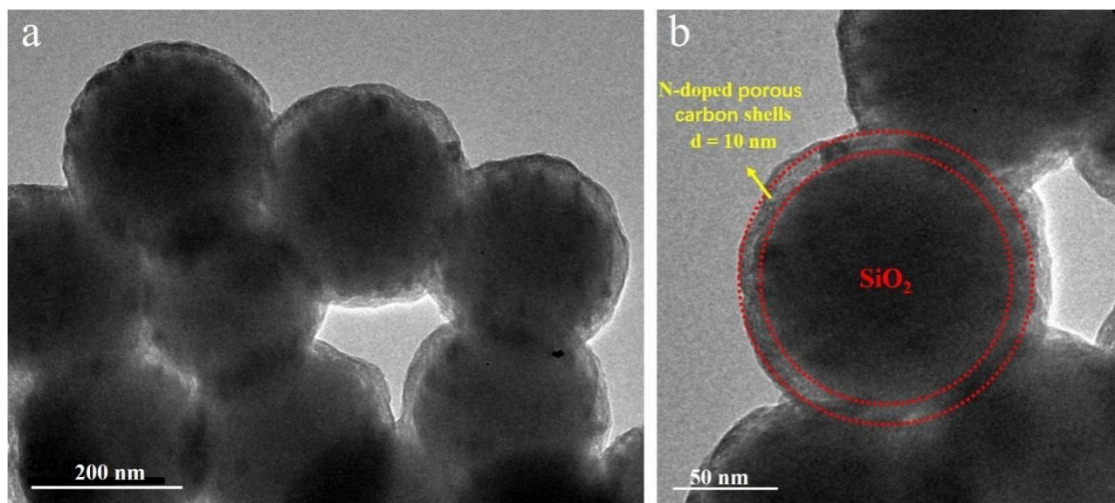


**Figure S3.** TEM images of SiO<sub>2</sub>@Co<sub>3</sub>O<sub>4</sub>@N-PCSs nanospheres.

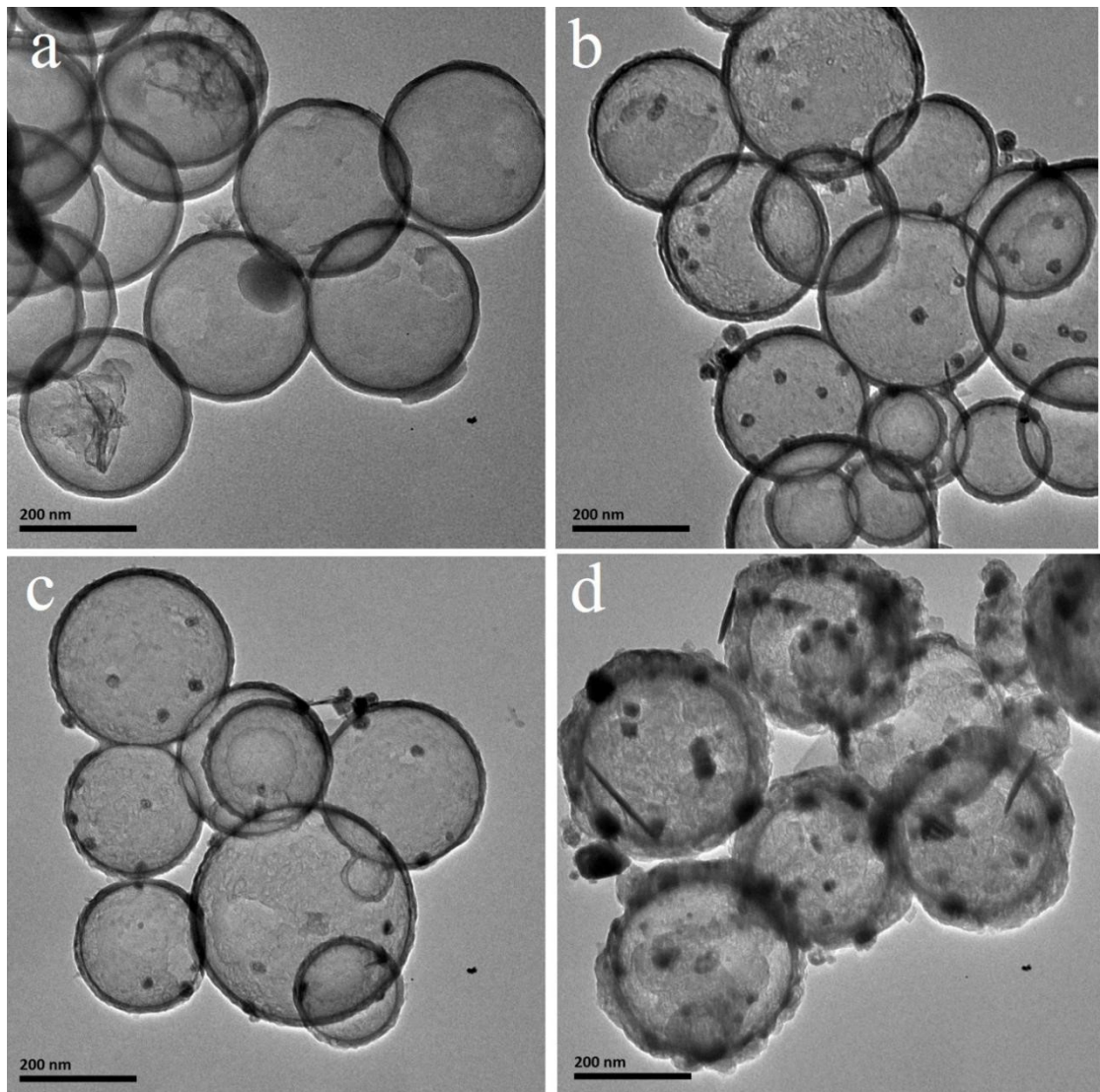


**Figure S4.** TEM images of a) N-HPCNsS, b)  $\text{Co}_3\text{O}_4$ -5%@N-HPCNs, c)  $\text{Co}_3\text{O}_4$ -10%@N-HPCNs and d)  $\text{Co}_3\text{O}_4$ -15%@N-HPCNs.

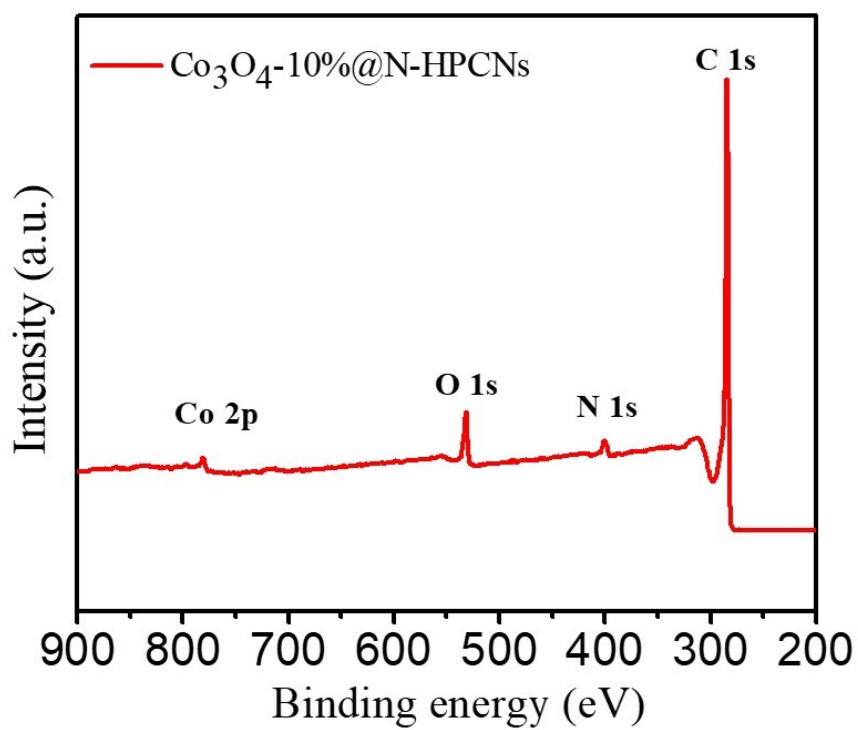


**Figure S5.** XPS survey spectrums of  $\text{Co}_3\text{O}_4$ -10%@N-HPCNs

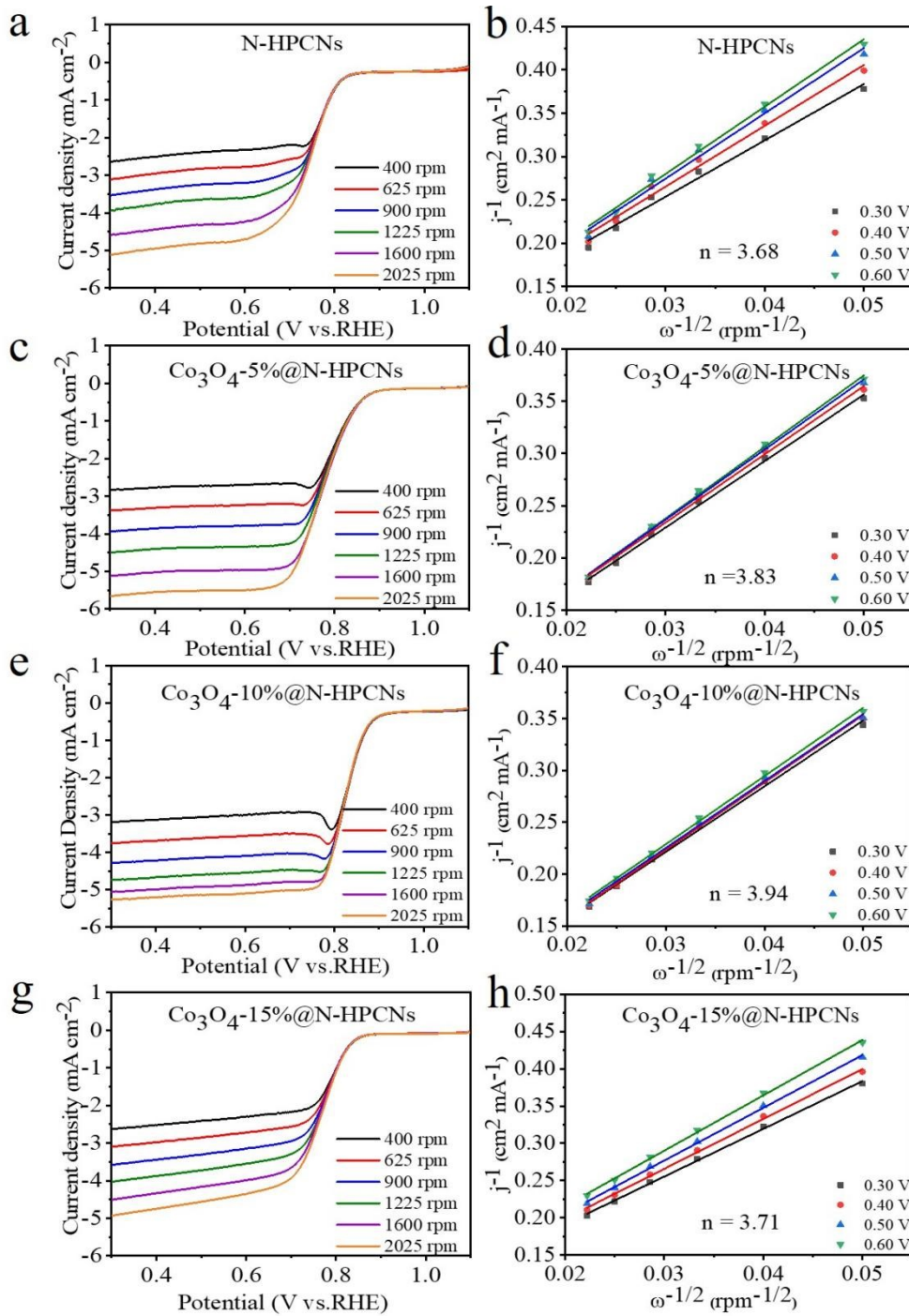


**Figure S6.** The RDE measurements of a) N-HPCNs, c)  $\text{Co}_3\text{O}_4\text{-}5\%@\text{N-HPCNs}$ , e)  $\text{Co}_3\text{O}_4\text{-}10\%@\text{N-HPCNs}$  and g)  $\text{Co}_3\text{O}_4\text{-}15\%@\text{N-HPCNs}$  at a scan rate of  $10 \text{ mV s}^{-1}$ , The Koutecky-Levich (K-L) plots of b) N-HPCNs, d)  $\text{Co}_3\text{O}_4\text{-}5\%@\text{N-HPCNs}$ , f)  $\text{Co}_3\text{O}_4\text{-}10\%@\text{N-HPCNs}$  and h)  $\text{Co}_3\text{O}_4\text{-}15\%@\text{N-HPCNs}$ .

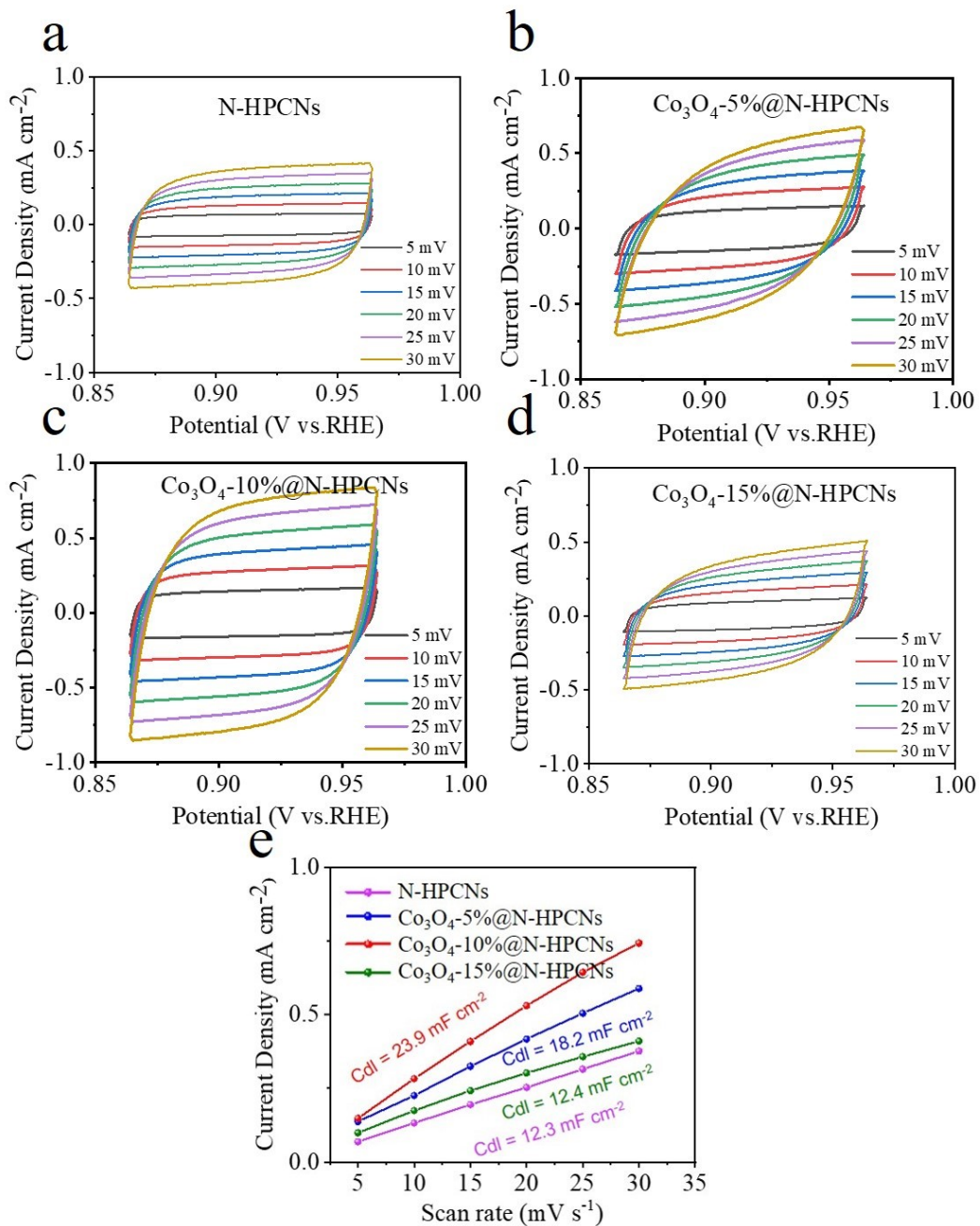


**Figure S7.** Scan rate dependence of current densities in CV curves for different electrocatalysts for ORR. a) N-HPCNs, b)  $\text{Co}_3\text{O}_4\text{-}5\%@\text{N-HPCNs}$ , c)  $\text{Co}_3\text{O}_4\text{-}10\%@\text{N-HPCNs}$ , d)  $\text{Co}_3\text{O}_4\text{-}15\%@\text{N-HPCNs}$ , e) Calculated  $C_{dl}$  values for all samples.

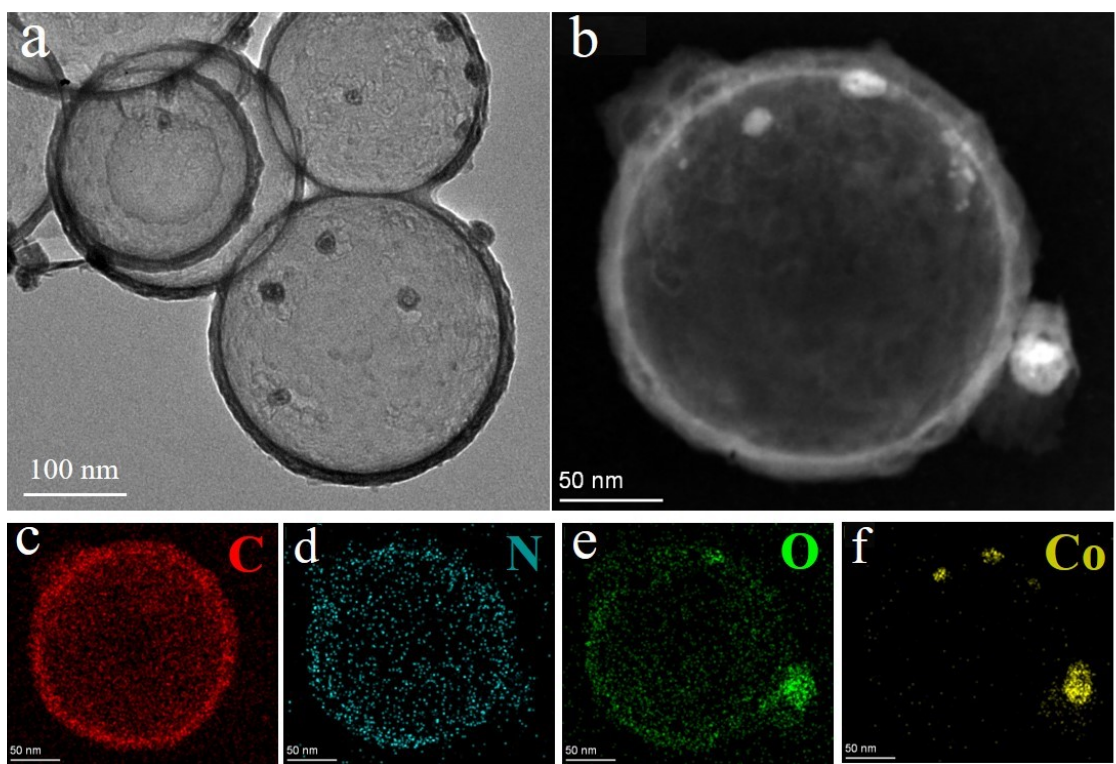


**Figure S8.** a) TEM and (b-f) EDS mapping images of HAADF-STEM elemental mapping images of  $\text{Co}_3\text{O}_4$ -10%@N-HPCNs after long-term ORR and OER stability tests.

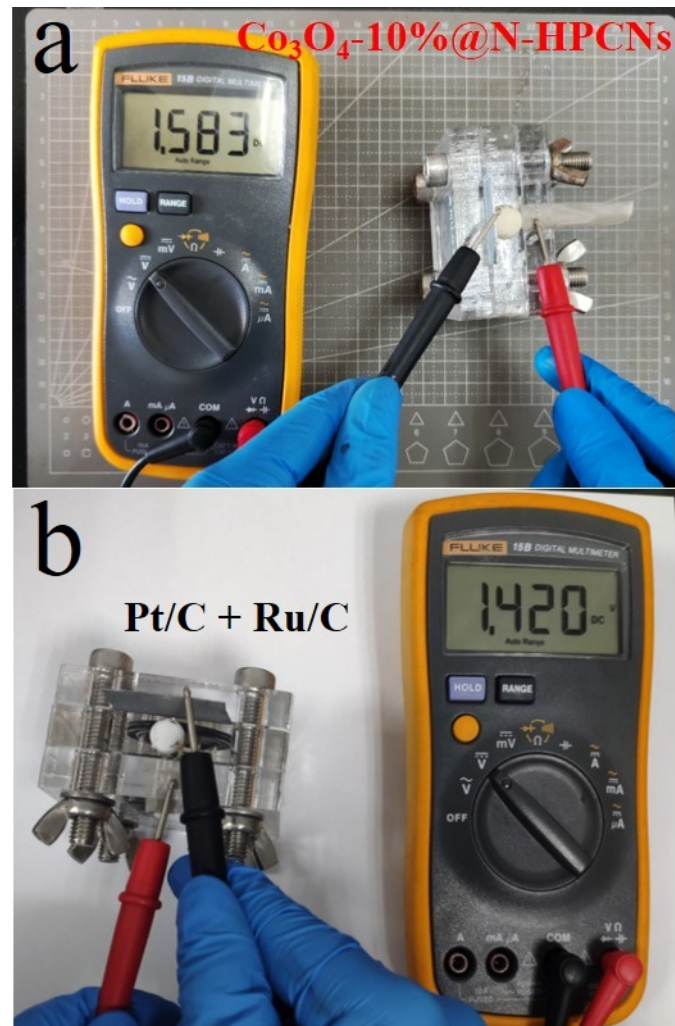


**Figure S9.** Photographs of open-circuit voltage of RZABs based on a)  $\text{Co}_3\text{O}_4\text{-}10\%\text{@N-HPCNs}$  and b)  $\text{Pt/C} + \text{Ru/C}$ .

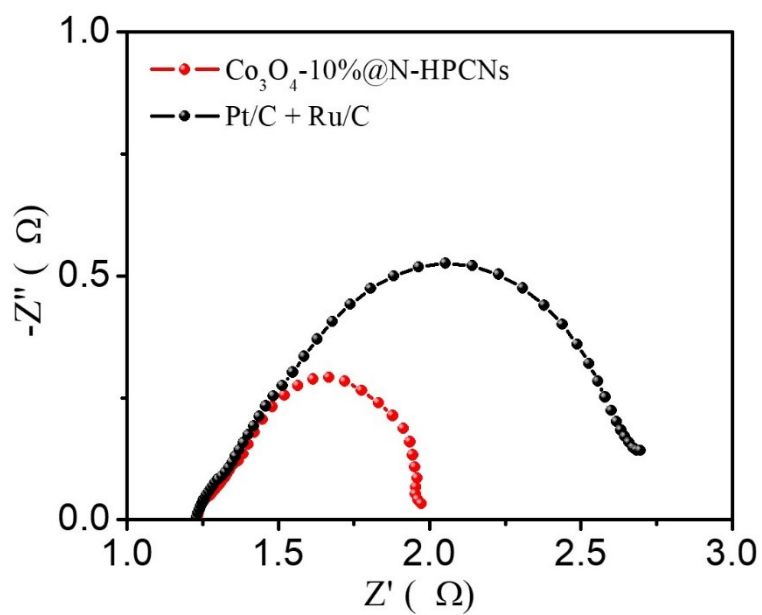


**Figure S10.** Nyquist plots of the RZABs based on  $\text{Co}_3\text{O}_4\text{-}10\%@\text{N-HPCNs}$  and  $\text{Pt/C} + \text{Ru/C}$ .

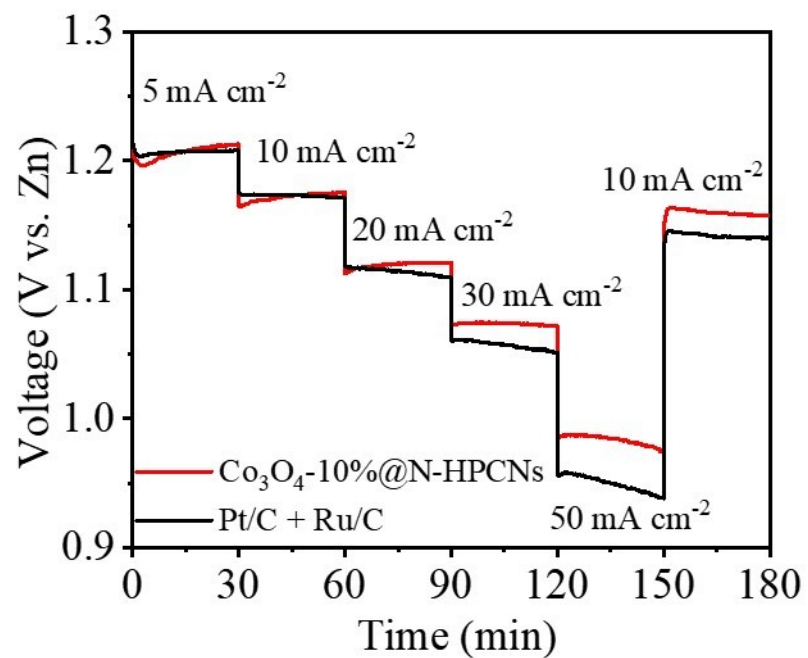


**Figure S11.** Discharge curves of the RZABs based on  $\text{Co}_3\text{O}_4$ -10%@N-HPCNs and Pt/C + Ru/C at various discharge current densities.

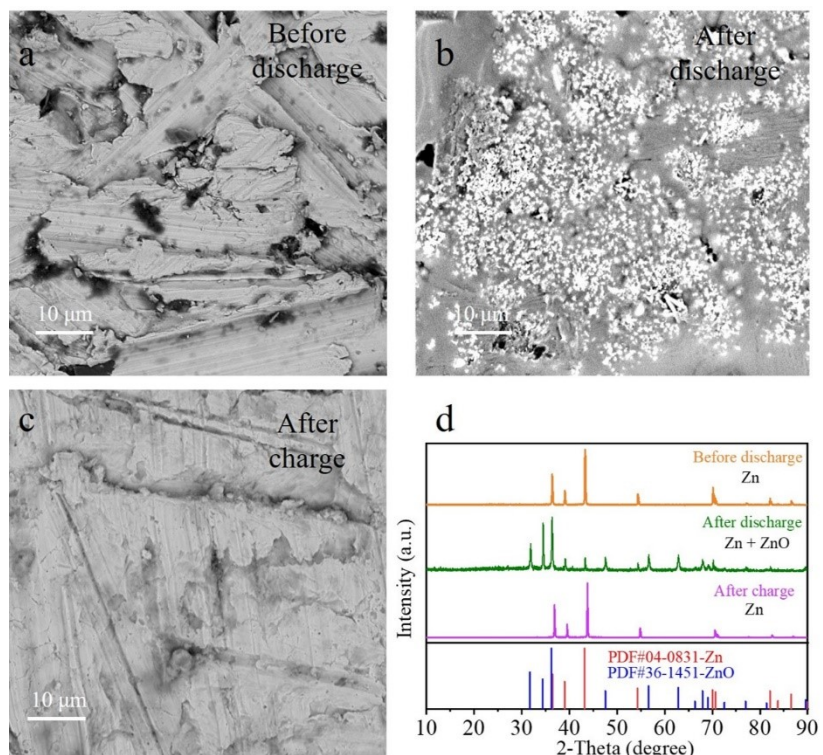


**Figure. S12** The SEM images of Zn anode a) before, b) after discharge and c) after charge, d) the XRD patterns of Zn anode before and after discharge and after charge.

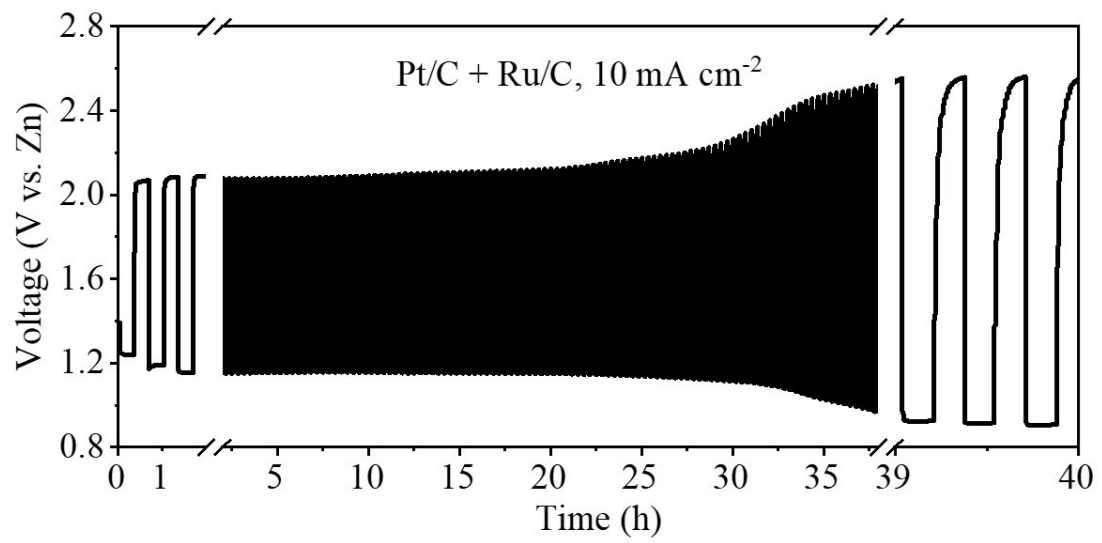


**Figure S13.** Galvanostatic cycling stability of RZABs with Pt/C + Ru/C cathode at a current density of  $10 \text{ mA cm}^{-2}$ .

**Table S1.** Thorough comparison of performances of recently reported bifunctional oxygen electrocatalysts.

Catalyst	ORR ( $E_{1/2}$ , V)	OER ( $E_{j=10}$ , V)	Activity ( $\Delta E = E_{j=10} - E_{1/2}$ , V)	Reference
<b>Co<sub>3</sub>O<sub>4</sub>-10%@N-HPNCs</b>	<b>0.83</b>	<b>1.61</b>	<b>0.78</b>	<b>This work</b>
Co-Co <sub>3</sub> O <sub>4</sub> @NAC	0.79	1.61	0.81	S1
Co <sub>3</sub> O <sub>4</sub> -Co/CoFe@C	0.81	1.59	0.78	S2
Co@Co <sub>3</sub> O <sub>4</sub> /NC	0.80	1.65	0.85	S3
Co <sub>9</sub> S <sub>8</sub> -NSHPCNF	0.82	1.58	0.76	S4
CoFe <sub>2</sub> O <sub>4</sub> @CNTs	0.78	1.74	0.96	S5
N-CNSP	0.85	1.62	0.77	S6
NiO/CoN PINWs	0.68	1.53	0.85	S7
Co <sub>7</sub> Fe <sub>3</sub> /CFNC	0.83	1.63	0.80	S8
Fe <sub>3</sub> C/Fe <sub>2</sub> O <sub>3</sub> @NGNs	0.76	1.69	0.93	S9
CNTs@(Fe,Co)PP-700	0.86	1.80	0.94	S10
Co <sub>2</sub> P/CoN-in-NCNTs	0.85	1.65	0.80	S11
p-CoNi@NSCs	0.81	1.65	0.84	S12
NiFe-LDH/Co,N-CNF	0.79	1.54	0.75	S13

Co@N-CNT	0.83	1.61	0.78	S14
Zn–Co–S NN/CFP	0.81	1.55	0.74	S15
FeCo-NCNFs-800	0.79	1.68	0.89	S16
ZnCoNC-0.1	0.84	1.75	0.91	S17
Co-NC@LDH	0.80	1.60	0.80	S18
CoFe/NGCT	0.79	1.67	0.88	S19
CoNi/BCF	0.80	1.60	0.80	S20
Ni3Fe/N-C	0.76	1.60	0.84	S21
NCO/N-rGO	0.78	1.63	0.85	S22
Co@NPCFs	0.66	1.63	0.97	S23
CoNC-MOG-9	0.79	1.63	0.84	S24

Catalyst	Open circuit voltage (V)	power density (mW cm <sup>-2</sup> )	Stability of RZABs <sup>a</sup>	Reference
<b>Co<sub>3</sub>O<sub>4</sub>-10%@N-HPNCs</b>	<b>1.583</b>	<b>145</b>	<b>1000 h 10 mA cm<sup>-2</sup></b>	<b>This work</b>
Co-Co <sub>3</sub> O <sub>4</sub> @NAC	1.449	164	35 h 10 mA cm <sup>-2</sup>	S1
NiO/CoN PINWs	1.460	79.6	8 h 3 mA cm <sup>-2</sup>	S7
Co <sub>7</sub> Fe <sub>3</sub> /CFNC	1.446	100.6	260 h 10 mA cm <sup>-2</sup>	S8
CNTs@(Fe,Co)PP-700	1.537	74	116 h 2 mA cm <sup>-2</sup>	S10
Co <sub>2</sub> P/CoN-in-NCNTs	1.362	194.6	95 h 10 mA cm <sup>-2</sup>	S11
p-CoNi@NSCs	1.460	87.9	430 h 10 mA cm <sup>-2</sup>	S12
Co@N-CNT	1.450	168	9.5 h 20 mA cm <sup>-2</sup>	S14
FeCo-NCNFs-800	1.480	74	40 h 10 mA cm <sup>-2</sup>	S15
CoNi/BCF	1.438	155.1	30 h 10 mA cm <sup>-2</sup>	S20
Co@NPCFs	1.450	91.9	80 h 2 mA cm <sup>-2</sup>	S24
Co@NCNT-300	1.521	162.5	0.6 h 10 mA cm <sup>-2</sup>	S25
Co-SAs@NC	1.460	105.3	85 h 10 mA cm <sup>-2</sup>	S26
FeCo@MNC	1.410	143	48 h 20 mA cm <sup>-2</sup>	S27
Fe/Co-N/S-C	1.395	102.6	26.7 h 5 mA cm <sup>-2</sup>	S28

FeCoMoS@NG	1.440	118	$70\text{ h}$ $2\text{ mA cm}^{-2}$	S29
CoFe@NC-SE	1.581	102	$30\text{ h}$ $5\text{ mA cm}^{-2}$	S30
Co@NGC-NSs	1.360	52.3	$16\text{ h}$ $5\text{ mA cm}^{-2}$	S31
N-HCNT-70	1.492	189.3	$84\text{ h}$ $10\text{ mA cm}^{-2}$	S32
CoO/NG	1.490	169.6	$40\text{ h}$ $10\text{ mA cm}^{-2}$	S33

<sup>a</sup>The cycling conditions and period of rechargeable Zn-air batteries.

## References

- S1. X. Zhong, W. Yi, Y. Qu, L. Zhang, H. Bai, Y. Zhu, J. Wan, S. Chen, M. Yang, L. Huang, M. Gu, H. Pan and B. Xu, *Appl. Catal. B*, 2020, **260**, 118188.
- S2. T. Li, Y. Lu, S. Zhao, Z. Gao and Y. Song, *J. Mater. Chem. A*, 2018, **6**, 3730-3737.
- S3. A. Ajaz, J. Masa, C. Rosler, W. Xia, P. Weide, A. J. Botz, R. A. Fischer, W. Schuhmann and M. Muhler, *Angew. Chem. Int. Ed.*, 2016, **55**, 4087-4091.
- S4. W. Peng, Y. Wang, X. Yang, L. Mao, J. Jin, S. Yang, K. Fu and G. Li, *Appl. Catal. B*, 2020, **268**, 118437.
- S5. N. Xu, J. Qiao, Q. Nie, M. Wang, H. Xu, Y. Wang and X.-D. Zhou, *Catal. Today*, 2018, **318**, 144-149.
- S6. L. Zong, W. Wu, S. Liu, H. Yin, Y. Chen, C. Liu, K. Fan, X. Zhao, X. Chen, F. Wang, Y. Yang, L. Wang and S. Feng, *Energy Stor. Mater.*, 2020, **27**, 514-521.
- S7. J. Yin, Y. Li, F. Lv, Q. Fan, Y. Q. Zhao, Q. Zhang, W. Wang, F. Cheng, P. Xi and S. Guo, *ACS Nano*, 2017, **11**, 2275-2283.
- S8. T. Tu, X. Zhou, P. Zhang, L. Tan, Z. Xu, M. Liu, W. Li, X. Kang, Y. Wu and J. Zheng, *ACS Sustainable Chem. Eng.*, 2022, **10**, 8694-8703.
- S9. Y. Tian, L. Xu, J. Qian, J. Bao, C. Yan, H. Li, H. Li and S. Zhang, *Carbon*, 2019, **146**, 763-771.
- S10. Y. Qi, S. Yuan, L. Cui, Z. Wang, X. He, W. Zhang and T. Asefa, *ChemCatChem*, 2020, **13**, 1023-1033.
- S11. Y. Guo, P. Yuan, J. Zhang, H. Xia, F. Cheng, M. Zhou, J. Li, Y. Qiao, S. Mu and Q. Xu, *Adv. Funct. Mater.*, 2018, **28**, 1805641.
- S12. X. He, J. Fu, M. Niu, P. Liu, Q. Zhang, Z. Bai and L. Yang, *Electrochim. Acta*, 2022, **413**, 140183.
- S13. Q. Wang, L. Shang, R. Shi, X. Zhang, Y. Zhao, G. I. N. Waterhouse, L. Wu, C. Tung and T. Zhang, *Adv. Energy Mater.*, 2017, **7**, 1700467.
- S14. Q. Dong, H. Wang, S. Ji, X. Wang, Z. Mo, V. Linkov and R. Wang, *Chem. Eur. J.*, 2020, **26**, 10752-10758.
- S15. X. Wu, X. Han, X. Ma, W. Zhang, Y. Deng, C. Zhong and W. Hu, *ACS Appl. Mater. Interfaces*, 2017, **9**, 12574-12583.
- S16. L. Yang, S. Feng, G. Xu, B. Wei and L. Zhang, *ACS Sustainable Chem. Eng.*, 2019, **7**, 5462-5475.
- S17. X. Wu, G. Meng, W. Liu, T. Li, Q. Yang, X. Sun and J. Liu, *Nano Research*, 2017, **11**, 163-173.
- S18. D. Chen, X. Chen, Z. Cui, G. Li, B. Han, Q. Zhang, J. Sui, H. Dong, J. Yu, L. Yu and L. Dong, *Chem. Eng. J.*, 2020, **399**, 125718.
- S19. X. Liu, L. Wang, P. Yu, C. Tian, F. Sun, J. Ma, W. Li and H. Fu, *Angew. Chem. Int. Ed.*, 2018, **57**, 16166-16170.
- S20. W. Wan, X. Liu, H. Li, X. Peng, D. Xi and J. Luo, *Appl. Catal. B*, 2019, **240**, 193-200.
- S21. G. Fu, Z. Cui, Y. Chen, Y. Li, Y. Tang and J. B. Goodenough, *Adv. Energy Mater.*, 2017, **7**, 1601172.
- S22. P. Moni, S. Hyun, A. Vignesh and S. Shanmugam, *Chem. Commun. (Cambridge, U. K.)*, 2017, **53**, 7836-7839.

- S23. Y. Chen, W. Zhang, Z. Zhu, L. Zhang, J. Yang, H. Chen, B. Zheng, S. Li, W. Zhang, J. Wu and F. Huo, *J. Mater. Chem. A*, 2020, **8**, 7184-7191.
- S24. N. Shang, S. Li, X. Zhou, S. Gao, Y. Gao, C. Wang, Q. Wu and Z. Wang, *Appl. Surf. Sci.*, 2021, **537**, 147818.
- S25. P. Rao, P. Cui, L. Yang, M. Wang, S. Wang, H. Cai, Y. Wang, X. Zhao, D. P. Wilkinson and J. Zhang, *J. Power Sources*, 2020, **453**, 227858.
- S26. X. Han, X. Ling, Y. Wang, T. Ma, C. Zhong, W. Hu and Y. Deng, *Angew. Chem. Int. Ed.*, 2019, **58**, 5359-5364.
- S27. C. Li, M. Wu and R. Liu, *Appl. Catal. B*, 2019, **244**, 150-158.
- S28. C. Li, H. Liu and Z. Yu, *Appl. Catal. B*, 2019, **241**, 95-103.
- S29. S. Ramakrishnan, J. Balamurugan, M. Vinothkannan, A. R. Kim, S. Sengodan and D. J. Yoo, *Appl. Catal. B*, 2020, **279**, 119381.
- S30. A. Samanta and C. R. Raj, *J. Power Sources*, 2020, **455**.
- S31. P. Thakur, M. Yeddala, K. Alam, S. Pal, P. Sen and T. N. Narayanan, *ACS Appl. Energy Mater.*, 2020, **3**, 7813-7824.
- S32. E. Y. Choi, D. E. Kim, S. Y. Lee and C. K. Kim, *Carbon*, 2020, **166**, 245-255.
- S33. L. Xu, C. Wang, D. Deng, Y. Tian, X. He, G. Lu, J. Qian, S. Yuan and H. Li, *ACS Sustainable Chem. Eng.*, 2019, **8**, 343-350.